CSIRO PUBLISHING

Aust. J. Chem. **2013**, *66*, 1406–1414
http://dx.doi.org/10.1071/CH13329

Full Paper

Synthesis and Characterisation of Ru^{II} Polypyridyl Complexes: DNA-Binding, Photocleavage, and Topoisomerase I and II Inhibitory Activity

Xiaojun He,[A,C] *Guang Yang,*[A,C] *Xiaonan Sun,*[A] *Lingjun Xie,*[A] *and Lifeng Tan*[A,B,D]

[A]College of Chemistry, Xiangtan University, Xiangtan 411105, China.
[B]Key Lab of Environment-friendly Chemistry and Application in Ministry of Education, Xiangtan University, Xiangtan 411105, China.
[C]These two authors are both first authors.
[D]Corresponding author. Email: lfwyxh@yahoo.com.cn

Two mixed-ligand ruthenium(II) complexes $[Ru(phen)_2(cptcp)]^{2+}$ (Ru**1**; phen = 1,10-phenanthroline, cptcp = 2-(4-carbazol-9-yl-phenyl)-1*H*-1,3,7,8-tetraaza-cyclopenta-[*l*]-phenanthrene) and $[Ru(phen)_2(btcpc)]^{2+}$ (Ru**2**; btcpc = 9-butyl-6-(1*H*-1,3,7,8-tetraaza-cyclo-cyclopenta-[*l*]-phenanthren-2-yl)-9*H*-carbazole-3-carbaldehyde) have been synthesised and characterised. The DNA-binding behaviours of the two complexes have been investigated by using spectroscopic and viscosity measurements. Results suggest that the two complexes bind to DNA by intercalation. The photocleavage of plasmid pBR322 DNA indicates that Ru**1** exhibits more effective DNA cleavage activity in comparison to that exhibited by Ru**2** under the same conditions, and different cleavage mechanisms are determined. Topoisomerase inhibition and DNA strand passage assay confirm that Ru**1** may act as an efficient dual inhibitor of topoisomerases I and II, whereas Ru**2** may only act as a single inhibitor of topoisomerases II.

Manuscript received: 27 June 2013.
Manuscript accepted: 23 July 2013.
Published online: 20 August 2013.

Introduction

DNA topoisomerases are crucial nuclear enzymes that regulate the topological state of DNA during replication, transcription, recombination, and chromosome segregation at mitosis.[1] Two types of DNA topoisomerases have been isolated from prokaryotes and eukaryotes. In general, topoisomerase I (Topo I) catalyses the relaxation of superhelical DNA generating a transient single strand nick in the DNA duplex,[2] whereas topoisomerase II (Topo II) mediates the ATP-dependent induction of coordinated nicks in both strands of the DNA duplex.[3] Under normal conditions, the step of DNA relegation is much faster than that of DNA cleavage, which may be tolerated by the cell. However, conditions that significantly change either the physiological concentration or the lifetime of the breaks are responsible for DNA alterations, playing a crucial role in inhibiting cell cycle progression.[4] Thus, inhibition of topoisomerases has been considered as an effective strategy for the design of many anticancer agents.[5]

In recent years, numerous natural and synthetic compounds have been chosen to detect the inhibition of topoisomerase activity.[2a,6] Most of such studies at present, however, have mainly revolved around organic compounds and, to a far lesser extent, around metal complexes.[6f,7] Metal complexes with a coordination centre have many advantages over organic molecules, such as a larger variety of structures, higher environmental stability, and a much greater diversity of tunable electronic properties.

During the past decade, the interest in the field of Ru^{II} polypyridyl complexes–nucleic acid interactions has burgeoned due to Ru^{II} polypyridyl complexes with rich photochemical properties and varied coordination forms.[8] However, surprisingly, and in contrast to studies on Ru^{II} polypyridyl complexes–nucleic acid interactions, investigations of the inhibition of topoisomerases activity by Ru^{II} polypyridyl complexes and the relationship between the structures of Ru^{II} complexes and the enzymatic inhibition activities are very scarce.[6f]

In addition, the emergence of resistance phenomena to Topo I inhibitors is often accompanied by a concomitant rise of the level of Topo II expression and vice-versa, resulting in the failure of clinical therapies.[4] In this regard, a single compound able to inhibit both Topo I and II may present the advantage of improving antitopoisomerase activity, with reduced toxic side effects, with respect to the combination of two inhibitors.[9] Recently, although some DNA-intercalating Ru^{II} polypyridyl complexes exhibited inhibition activities on Topo II,[7e,8a,10] studies involving the dual inhibition of Topo I and II by Ru^{II} polypyridyl complexes are very scarce.[8c,11] Therefore, studies on the interaction between polypyridyl-based Ru^{II} complexes and topoisomerases are very important for developing novel antitumour drugs and elucidating the underlying molecular mechanism.

Considering all the above, two new Ru^{II} polypyridyl complexes (Fig. 1), $[Ru(phen)_2(cptcp)]^{2+}$ (Ru**1**; phen = 1,10-phenanthroline, cptcp = 2-(4-carbazol-9-yl-phenyl)-1*H*-1,3,7,8-tetraaza-cyclopenta-[*l*]-phenanthrene) and $[Ru(phen)_2(btcpc)]^{2+}$

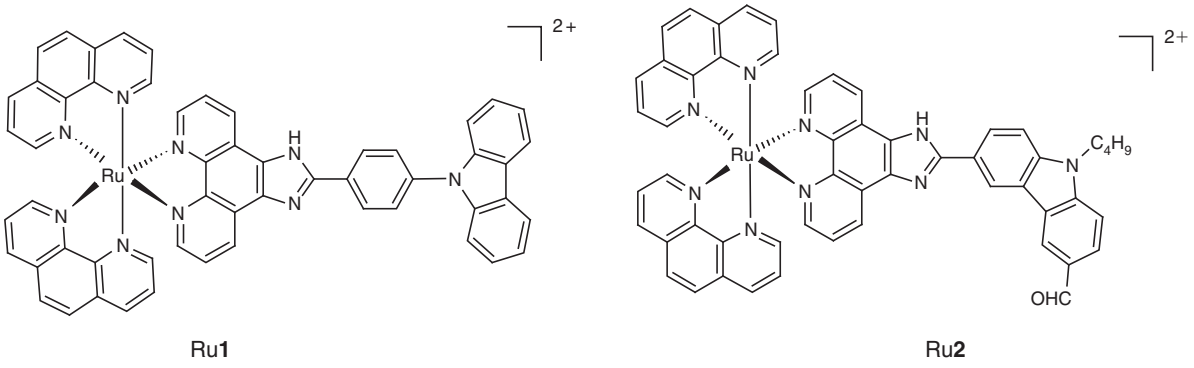

Fig. 1. Chemical structures of Ru**1** and Ru**2**.

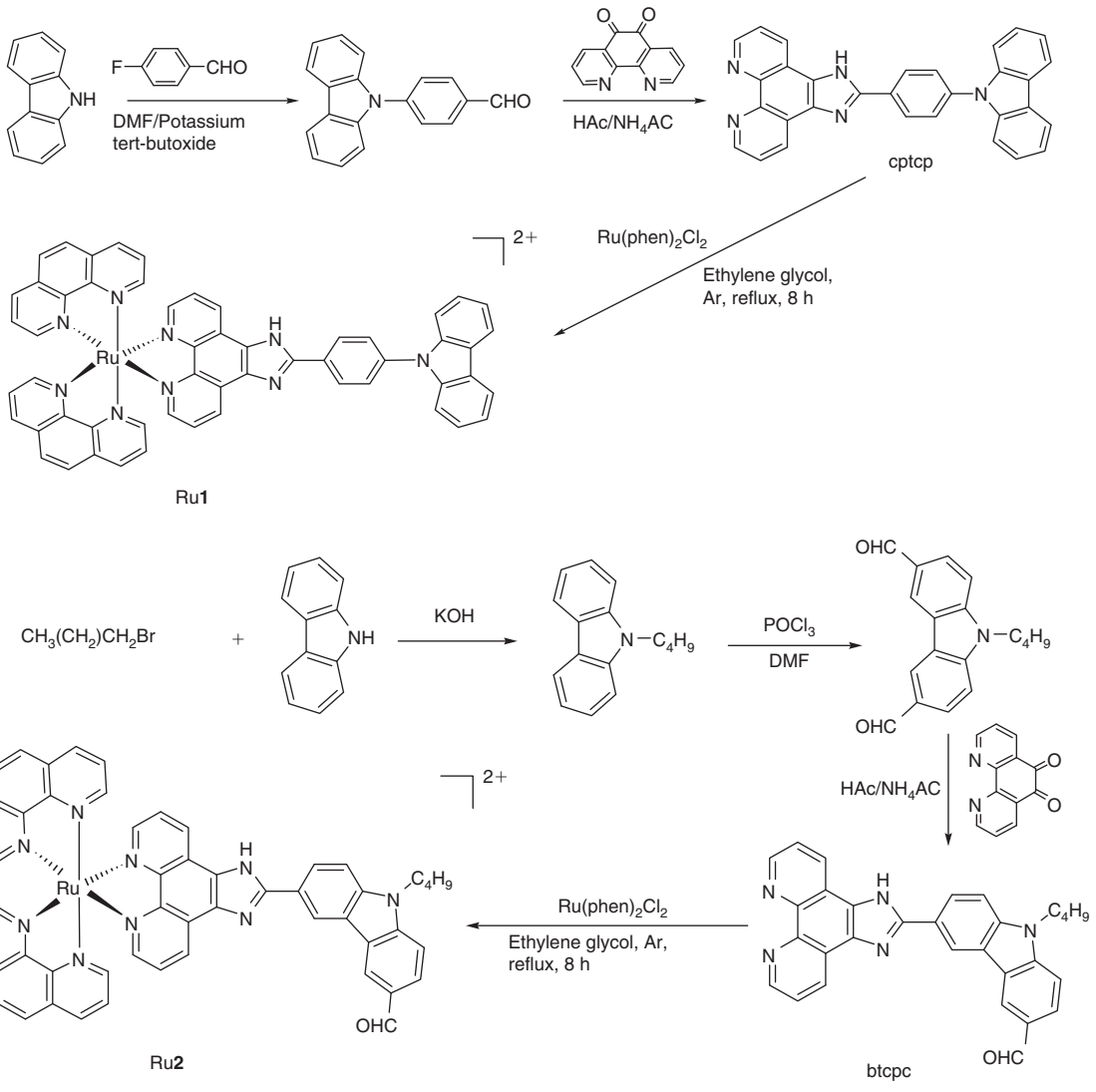

Scheme 1. Synthesis of the ligands cptcp (2-(4-carbazol-9-yl-phenyl)-1*H*-1,3,7,8-tetraaza-cyclopenta-[*l*]-phenanthrene) and btcpc (9-butyl-6-(1*H*-1,3,7,8-tetraaza-cyclo-cyclopenta-[*l*]-phenanthren-2-yl)-9*H*-carbazole-3-carbaldehyde) and their complexes Ru**1** and Ru**2**.

(Ru**2**; btcpc = 9-butyl-6-(1*H*-1,3,7,8-tetraaza-cyclopenta-[*l*]-phenanthren-2-yl)-9*H*-carbazole-3-carbaldehyde) have been synthesised and characterised. The DNA binding, DNA photocleavage, and topoisomerase inhibitory activity of the two complexes have been analysed.

Results and Discussion

Synthesis and Characterisation

The synthetic routes to cptcp, btcpc, and their Ru^{II} complexes are shown in Scheme 1. According to protocols reported by

Steck and Day,[12] cptcp and btcpc were synthesised by coupling 1,10-phenanthroline-5,6-dione with 4-carbazol-9-yl-benzaldehyde and 9-butyl-9*H*-carbazole-3,6-dicarbaldehyde, respectively. Using a mixture of water and ethanol as solvent, Ru**1** and Ru**2** were prepared by direct reaction of the precursor complex *cis*-$[Ru(phen)_2Cl_2]\cdot 2H_2O$ with the appropriate mole ratios of cptcp and btcpc, and were obtained in yields of 67 and 62 %, respectively. The desired Ru^{II} complexes were isolated as their perchlorates and then purified by column chromatography to afford satisfactory purity, which was verified by elemental analysis, matrix-assisted laser desorption ionisation time-of-flight (MALDI-ToF) mass spectrometry (Fig. S1 in the Supplementary Material), and NMR spectroscopy (Fig. S2 in the Supplementary Material).

The absorption spectra of Ru**1** and Ru**2** (Fig. S3 in the Supplementary Material) in acetonitrile are very similar and consist of three well resolved bands at ~460, 350, and 264 nm. The bands at ~350 and 264 nm are attributed to intraligand (IL) $\pi \rightarrow \pi^*$ transitions.[13] The lowest energy band, at ~460 nm, is assigned to a metal–ligand charge transfer (MLCT) transition, which is attributed to Ru(dπ) → cptcp or btcpc (π^*) transitions. In comparison to the spectra of other polypyridyl Ru^{II} complexes, such as $[Ru(phen)_3]^{2+}$ (λ_{max} 448 nm),[13] $[Ru(bpy)_2(ip)]^{2+}$ (λ_{max} 455 nm), $[Ru(bpy)_2(pip)]^{2+}$ (λ_{max} 458 nm) (where bpy = 2,2′-bipyridine, ip = imidazo[4,5-*f*] [1,10]-phenanthroline, and pip = 2-phenylimidazo[4,5-*f*]1,10-phenanthroline),[14] the MLCT bands of Ru**1** and Ru**2** are obviously red shifted, which may be due to the increased π delocalisation and, thus, the π-acceptor capacity of the ligands btcpc and cptcp, resulting in a decreased electron density on the central Ru^{II} and, in turn, stabilisation of the metal dπ orbital.

Complexes Ru**1** and Ru**2**, upon dissolution in various solvents, such as acetonitrile and water, could emit luminescence in the absence of DNA at 25°C. As shown in Fig. S4 in the Supplementary Material, Ru**1** and Ru**2** showed emission in acetonitrile with a maximum appearing at 597 and 585 nm, respectively. Note that distinct red shifts around 12 nm were observed for Ru**1** and Ru**2** in aqueous solution. In addition, the emission spectra of Ru**1** and Ru**2** are somewhat solvatochromic, reflecting that the more polar the solvent, the smaller the relative intensity.[15,16]

Electronic Absorption Titration

The application of electronic absorption spectroscopy in DNA-binding studies is one of the most useful techniques.[17] Upon gradual addition of DNA, the electronic absorption spectroscopy of the complex is perturbed due to the stacking interactions between the aromatic chromophore of the intercalative ligand in the complex and the base pairs of DNA. Therefore, binding of the complex to DNA by intercalation usually results in hypochromism and bathochromism. In general, the extent of the hypochromism commonly parallels the intercalative binding strength. The absorption spectra of Ru**1** and Ru**2** in the absence and presence of calf thymus (CT)-DNA are given in Fig. 2. As the concentrations of DNA are increased to saturation, for Ru**1**, the hypochromism at 351 nm reaches as high as 14.1 % with a red shift of 4 nm at a [DNA]/[Ru] ratio of 2.31; for Ru**2**, the hypochromism at 367 nm reaches ~9.8 % with a red shift of 2 nm at a [DNA]/[Ru] ratio of 3.55. These spectroscopic characteristics obviously suggest that both complexes can interact with DNA, which most likely proceeds through a mode that involves a stacking interaction between the aromatic chromophore and the base pairs of DNA.

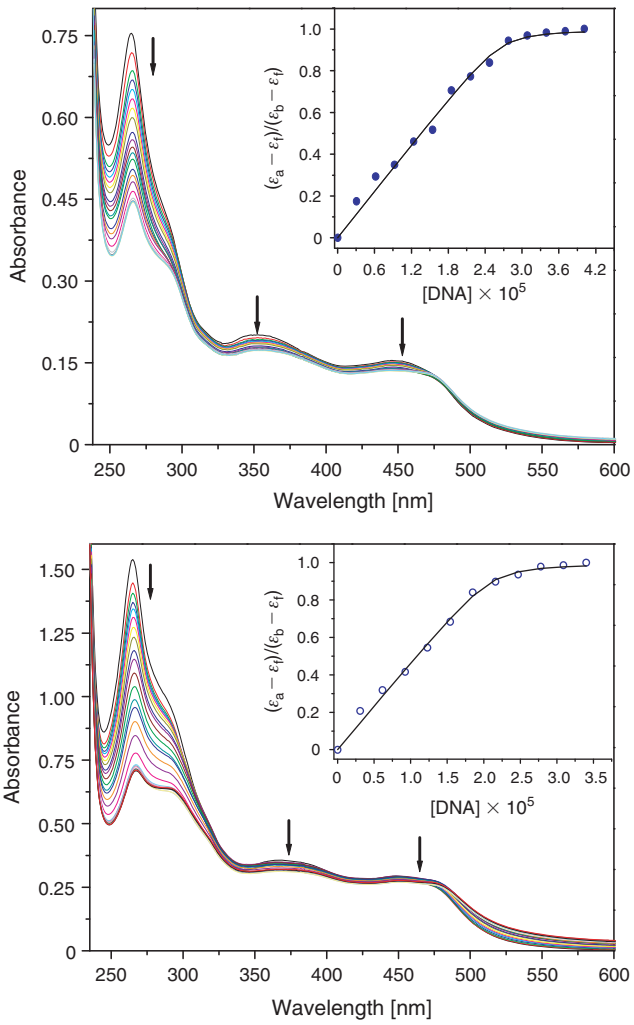

Fig. 2. Absorption spectra of Ru**1** (top) and Ru**2** (bottom) in Tris–HCl buffer upon addition of calf thymus (CT)-DNA. [Ru**1**] = 10 μM, [Ru**2**] = 20 μM, [DNA] = 0–34 μM. Arrow shows the absorbance changing upon the increase of DNA concentration. Inserts: plots of $(\varepsilon_a - \varepsilon_f)/(\varepsilon_b - \varepsilon_f)$ *v.* [DNA] for the titration of DNA to complexes Ru**1** and Ru**2**. ε_a, ε_f and ε_b are the apparent, free, and bound metal complex extinction coefficients, respectively.

From the decrease of the absorbance of both complexes (at 351 nm for Ru**1** and 367 nm for Ru**2**), the intrinsic binding constants K_b of Ru**1** and Ru**2** to DNA were determined as $(6.8 \pm 0.45) \times 10^6\,M^{-1}$ ($s = 0.67 \pm 0.15$), and $(4.61 \pm 0.22) \times 10^6\,M^{-1}$ ($s = 0.53 \pm 0.12$), respectively. The K_b values of the two complexes are comparable to that of $[Ru(bpy)_2(pip)]^{2+}$,[14] $[Ru(bpy)_2(ppd)]^{2+}$ (where ppd = pteridino [7,6-*f*][1,10]phenanthroline-1,13(10*H*,12*H*)-dione),[16] and the known DNA intercalator ethidium bromide (EB).[18] However, the K_b values of Ru**1** and Ru**2** are stronger than their parent complexes, $[Ru(bpy)_3]^{2+}$ ($4.7 \times 10^3\,M^{-1}$) and $[Ru(phen)_3]^{2+}$ ($5.4 \times 10^3\,M^{-1}$).[19] These data indicate that the size and the shape of the intercalated ligand of the Ru^{II} complexes have a significant effect on the strength of DNA binding, and the most suitable intercalating ligand leads to the highest affinity of complexes with DNA. Although the hydrophobicity of the intercalative ligand in Ru**2** is greater than that in Ru**1**, the steric hindrance caused by a normal-butyl group is not advantageous to the DNA-binding of Ru**2**, resulting in a lower DNA-binding affinity. Therefore, synthetically considering these factors, the

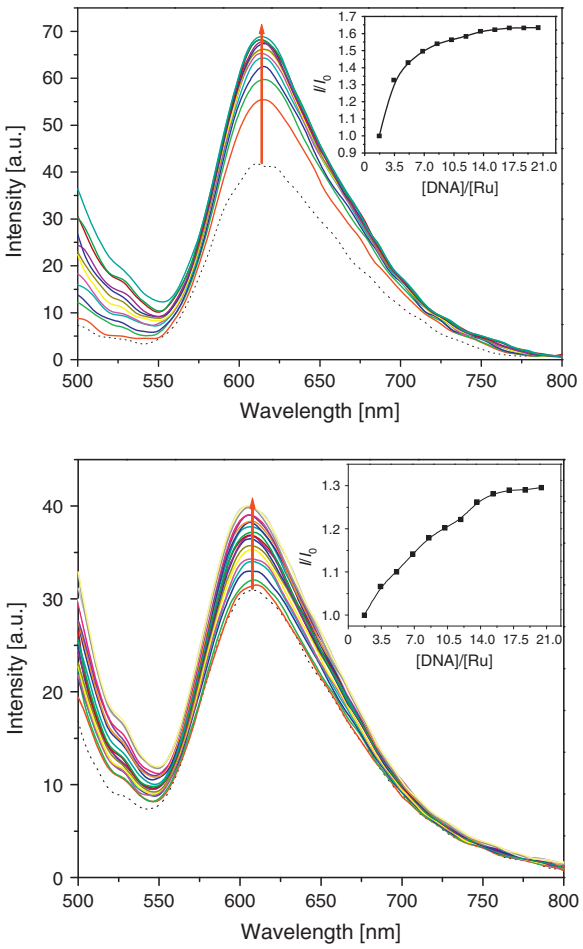

Fig. 3. Emission spectra of Ru**1** (top) and Ru**2** (bottom) in Tris–HCl buffer in the absence and presence of calf-thymus (CT)-DNA. Arrow shows the intensity change upon increasing DNA concentrations.

difference of the DNA-binding affinity of Ru**1** and Ru**2** can be well understood.

Luminescence Spectroscopic Studies

Luminescence spectroscopy is one of the most common and sensitive methods to analyse drug–DNA interactions. Support for the aforementioned intercalative binding mode also comes from the emission measurements of both complexes. In Tris–HCl buffer at 25°C, Ru**1** and Ru**2** showed fluorescence emission with a maximum appearing at ~600 nm in the absence of DNA (Fig. 3, dotted line). The emission spectroscopic changes of the two complexes upon increasing DNA concentrations are also given in Fig. 3 (solid lines). Fig. 3 indicates that the intrinsic fluorescence of either Ru**1** or Ru**2** grows steadily upon addition of DNA and eventually reaches 1.6 times or 1.3 times that of either Ru**1** or Ru**2** without DNA, which implies that the location of the bound Ru**1** and Ru**2** is in a hydrophobic environment similar to an intercalated state. The reason for this is that the hydrophobic environment inside DNA may reduce the accessibility of water molecules to the complex and the complex mobility is restricted at the binding site, leading to a decrease of the vibrational modes of relaxation in the excited state.[20] Compared with Ru**2**, the greater fluorescence changes in the presence of DNA are indicative of stronger association of Ru**1** to DNA. Therefore, Ru**1** is protected more efficiently than Ru**2** by DNA, resulting presumably from a more effective overlap of the

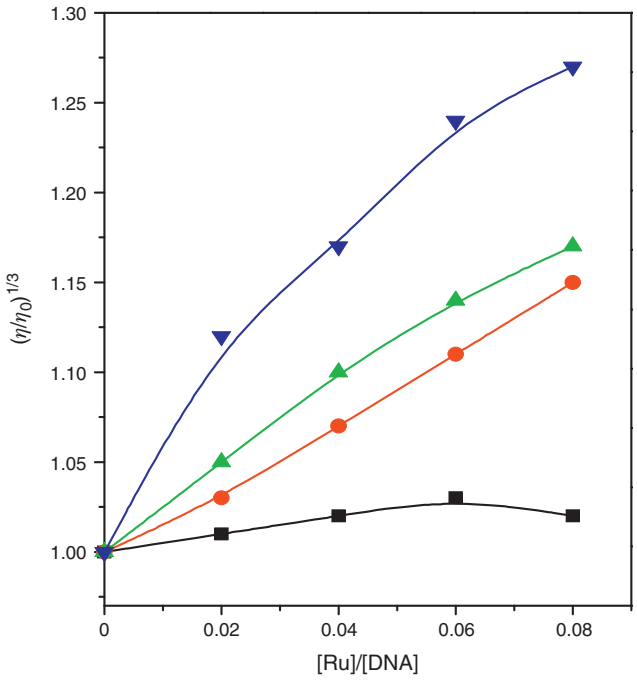

Fig. 4. Effect of increasing amounts of ethidium bromide (EB) (▼), $[Ru(bpy)_3]^{2+}$ (bpy = 2,2′–bipyridine) (■), Ru**1** (▲), and Ru**2** (●) on the relative viscosity of claf-thymus (CT)-DNA. Total DNA concentration: 0.5 mM, $T = 28 \pm 0.1$°C.

bound molecules with the base pairs of DNA. Regarding Ru**2**, the intercalative ligand btcpc containing a normal-butyl group is not advantageous to the interaction between btcpc and DNA, resulting in a lower DNA-binding affinity relative to Ru**1**.

Determination of the Binding Mode by Viscosity Studies

To further clarify the interactions between complexes and DNA, viscosity measurements were carried out on CT-DNA by varying the concentration of the added Ru^{II} complex. Hydrodynamic measurements that are sensitive to length change (i.e. viscosity and sedimentation) are regarded as the least ambiguous and the most critical tests of a binding model in solution in the absence of crystallographic structural data.[21] Fig. 4 indicates that upon increasing the concentrations of either Ru**1** or Ru**2**, the relative viscosity of DNA increases steadily, similar to the behaviour of EB. The increased degree of viscosity, which may depend on its affinity to DNA, follows the order of EB > Ru**1** > Ru**2** > $[Ru(bpy)_3]^{2+}$, suggesting that Ru**1** and Ru**2** bind to DNA by intercalation with different affinities. The difference of Ru**1** and Ru**2** binding with DNA could be caused by their different intercalative ligands. Obviously, the normal-butyl group in complex **2** is expected to give rise to steric hindrance, which is not advantageous to the DNA-binding of complex **2**. Thus, Ru**1** containing the intercalative ligand cptcp can intercalate more deeply into adjacent DNA base pairs than Ru**2** does, causing the helix to extend and the DNA viscosity to increase.

Thermal Denaturation Study

DNA melting experiments are useful to determine the extent of intercalation, because the intercalation of the complex into DNA base pairs causes stabilisation of the base stacking and, therefore, raises the melting temperature of the double-stranded DNA.[22] It is well accepted that when the temperature of the

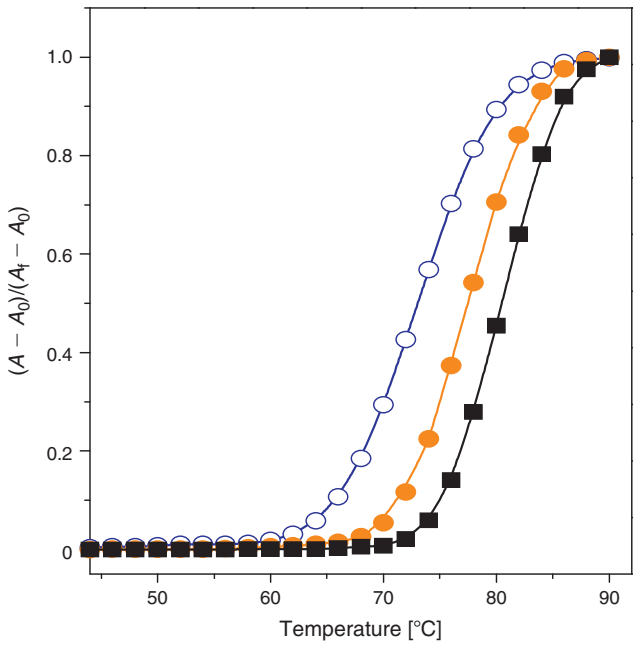

Fig. 5. Melting temperature curves of DNA in the absence (○) and presence of Ru**1** (●) and Ru**2** (■), respectively. [Ru] = 10 μM, [DNA] = 100 μM.

solution increases, the double-stranded DNA gradually dissociates into single strands, which generates a hyperchromic effect on the absorption spectra of the DNA bases (λ_{max} 260 nm). To identify this transition process, the melting temperature T_m, which is defined as the temperature where half of the total base pairs are unbonded, is usually introduced. According to previous reports,[23] the intercalation of a complex into DNA generally results in a considerable increase of T_m. The melting curve of CT-DNA in the absence and presence of either Ru**1** or Ru**2** is presented in Fig. 5. Here the T_m of metal complex-free CT-DNA was determined to be 73.17 ± 0.12°C. In the presence of either Ru**1** or Ru**2**, the T_m increases successively and reaches 82.81 ± 0.26 and 80.07 ± 0.33°C, respectively, at a [Ru]/[DNA] ratio of 1 : 10. The ΔT_m values (9.64 and 6.90°C) of Ru**1**/**2**–DNA adducts are larger than those of some Ru^{II} intercalators,[23] which reveals that the modes of both complexes binding to DNA are intercalation.

Photocleavage of pBR322 DNA by Ru^{II} Complexes

The cleavage reaction on plasmid DNA can be monitored by agarose gel electrophoresis. When circular plasmid DNA is subject to electrophoresis, relatively fast migration will be observed for the intact supercoil form (Form I). If scission occurs on one strand (nicking), the supercoil will relax to generate a slower moving open circular form (Form II). If both strands are cleaved, a linear form (Form III) that migrates between Form I and Form II will be generated.[24]

Fig. 6 shows the photoactivated cleavage of pBR322 DNA in the presence of different concentrations of either Ru**1** or Ru**2** after irradiation at 365 nm for 45 min. As seen in Fig. 6, control photoreactions with DNA alone ((a) and (b), lane 0) resulted in little or no DNA cleavage. In contrast, photoreactions using 365 nm ((a) and (b), lanes 1–5) resulted in different production of nicked DNA depending on the concentrations of both complexes used. For Ru**1**, at a concentration of 10 μM ((a), lane 5), approximately half of the supercoiled plasmid has been

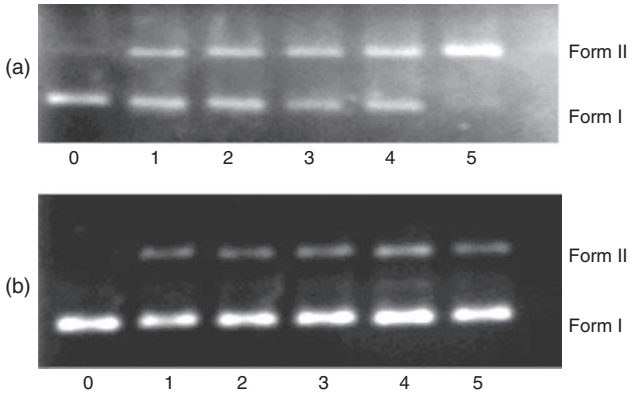

Fig. 6. Photoactivated cleavage of pBR322 DNA in the presence of (a) Ru**1** and (b) Ru**2**, after irradiation at 365 nm for 45 min. Lanes 0–5 are the different concentrations of either Ru**1** or Ru**2**: (0) 0; (1) 0.5; (2) 2.0; (3) 5.0; (4) 10; (5) 15 μM, respectively.

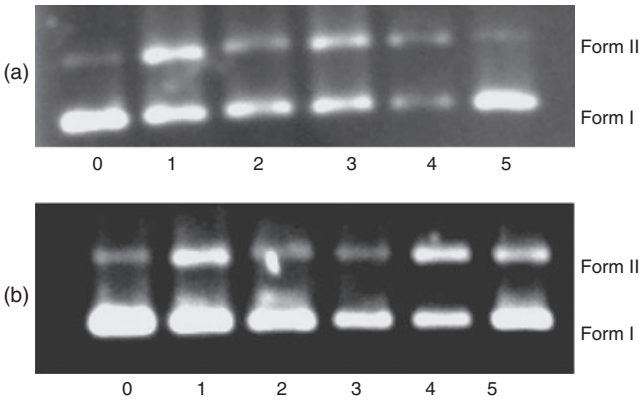

Fig. 7. Photoactivated cleavage of pBR322 in the presence of either (a) Ru**1** (10 μM) or (b) Ru**2** (10 μM) and different inhibitors after irradiation at 365 nm for 60 min. Lane 0, no complex; lane 1, no inhibitor; lanes 2–5: (2) in the presence of mannitol (100 mM); (3) in the presence of DMSO (10.0 mM); (4) in the presence of superoxide dismutase (1000 U mL^{-1}); and (5) in the presence of histidine (1.2 mM).

converted into nicked form; at a concentration of 15 μM ((a), lane 5), it can promote the complete conversion of DNA from Form I into Form II. However, the photoactivated cleavage of DNA is not sensitive to the concentrations of Ru**2**. Fig. 6 also indicates that even at a concentration of 15 μM, Ru**2** cannot promote the complete conversion of DNA from Form I into Form II. The results indicate that Ru**1** exhibits more effective DNA cleavage activity than Ru**2**.

In order to identify the nature of the reactive species that are responsible for the photoactivated cleavage of the plasmid DNA induced by either Ru**1** or Ru**2**, further investigations were carried out to evaluate the influence of different potentially inhibiting agents. In the case of Ru**1** (Fig. 7a), studies with the facile hydroxyl radical ($^{\bullet}OH$) scavengers mannitol and DMSO were carried out, and no obvious inhibition was observed (lanes 2 and 3), which indicated that the hydroxyl radical ($^{\bullet}OH$) was not the reactive species.[25] Similarly, in the presence of superoxide dismutase (SOD), a facile superoxide anion radical ($O_2^{\bullet-}$) quencher, no inhibition was observed (lane 4), this indicated that the superoxide anion radical ($O_2^{\bullet-}$) was not the reactive species either. However, in the presence of the singlet oxygen ($^1O_2$) quencher, histidine, obvious inhibition was observed (lane 5), which suggested that singlet oxygen ($^1O_2$) was involved in the

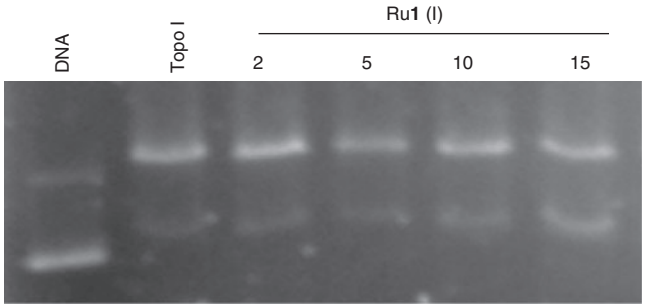

Fig. 8. Effects of different concentrations of Ru**1** on the activity of DNA Topo I.

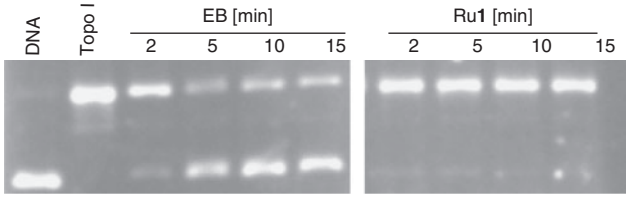

Fig. 9. The time dependence of Topo I DNA strand passage assays in the presence of ethidium bromide (EB) and Ru**1**.

cleavage.[26] On the contrary, for Ru**2** (Fig. 7b), the obvious inhibitions were observed in the presence of the facile hydroxyl radical (•OH) scavengers mannitol (lane 2) and DMSO (lane 3). This indicated that for Ru**2** the hydroxyl radical (•OH) plays a significant role in the photocleavage mechanism and the photoreduction of Ru^{II} complexes with concomitant hydroxide oxidation is an important step in the DNA cleavage reaction.[25]

Topoisomerases I and II Inhibition by Ru1 and Ru2

Topoisomerase inhibitory reactions were performed using Ru**1** and Ru**2**. Fig. 8 indicates that significant amounts of the supercoiled plasmid gradually increase upon increasing the concentrations of Ru**1**, which reflects that Ru**1** can inhibit the ability of Topo I to relax negatively supercoiled plasmid DNA by blocking the DNA strand passage event of the enzyme. For Ru**1**, the value of IC_{50} (half maximal inhibitory concentration) is ~15.4 μM. However, in the case of Ru**2** (Fig. S5 in the Supplementary Material), no obvious topoisomerase inhibitions are observed by increasing its concentrations from 0 to 20 μM, which indicates that Ru**2** can hardly inhibit the ability of Topo I to relax negatively supercoiled plasmid DNA at concentrations below 20 μM. The results suggest that Ru**1** may serve as a catalytic inhibitor of Topo I. Note that the complexes as DNA intercalators can induce constrained negative and unconstrained positive superhelical twists in plasmid DNA, resulting in directly altering the topological state of the negatively supercoiled DNA substrate. The reason for this is that Topo I could only remove the unconstrained positive supercoils. Therefore, the negatively supercoiled DNA product would be identical to the topological state of the original plasmid substrate. Thus, the inhibition of enzyme catalysis may also arise in the presence of the complexes as DNA intercalators.

To determine whether Ru**1** interferes with the DNA relaxation reaction by inhibiting Topo I catalysis or by altering the apparent topological state of DNA, the DNA strand passage assay was performed.[27] The effects of the complex on enzyme-catalysed DNA strand passage were assessed by comparing the rate of relaxation of negatively supercoiled plasmid without drug to the rate of supercoiling of the relaxed plasmid with EB. Fig. 9 indicated that the rate of supercoiling of relaxed plasmid in the presence of Ru**1** was much lower than that of relaxed plasmid in the presence of EB. EB is identical to the rate of Topo I-catalysed DNA relaxation in the absence of drug. The result reflected that Ru**1** was a Topo I poison, similar to that observed for other Ru^{II} complexes.[28]

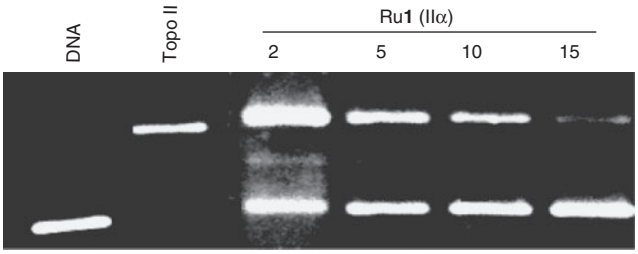

Fig. 10. Effects of different concentrations of Ru**1** on the activity of DNA Topo IIα.

The results of a concentration-dependent Topo II inhibition assay of Ru**1** and Ru**2** are given in Fig. 10 and Fig. S6 (Supplementary Material), respectively. As can be seen from Fig. 10 and Fig. S6, the amount of negatively supercoiled plasmid suffered different degrees of reduction upon increasing the concentrations of either Ru**1** or Ru**2**, which suggested that both complexes could inhibit the activity of Topo II. The value of IC_{50} for Topo II inhibition by Ru**1** is ~6.6 μM. However, for Ru**2**, its value of IC_{50} is smaller than 2 μM, suggesting that Ru**2** exhibits more effective Topo II inhibition activity than Ru**1** under the same conditions. Similar to that described above for Topo I, a DNA strand passage assay was also used to distinguish the effects of the complexes on Topo IIα function from their effects on DNA topology. As depicted in Fig. 11 and Fig. S7 (Supplementary Material), compared with the re-ligation rate of the relaxed plasmid in the presence of EB, the re-ligation rate of the relaxed plasmid in the presence of either Ru**1** or Ru**2** didn't slow down with the passage of time. The results indicate that Ru**1** and Ru**2** are suppressors of human topoisomerase IIα.

Conclusions

Two mixed-ligand Ru^{II} complexes $[Ru(phen)_2(cptcp)]^{2+}$ (Ru**1**) and $[Ru(phen)_2(btcpc)]^{2+}$ (Ru**2**) have been synthesised and characterised. The binding properties of the two complexes towards CT-DNA indicated that both complexes bind to CT-DNA by means of intercalation, while the binding affinity of Ru**1** with DNA is greater than that of Ru**2** with DNA. Ru**1** also exhibits more effective DNA cleavage activity than Ru**2** under the same condition. For Ru**1**, the singlet oxygen ($^1O_2$) is likely to be the reactive species responsible for the DNA cleavage, whereas the hydroxyl radical (•OH) may play a significant role in the DNA cleavage by Ru**2**. In addition, topoisomerases inhibition by the two complexes indicate that Ru**1** may serve as an efficient dual inhibitor of topoisomerases I and II, whereas Ru**2** may only act as a single inhibitor of topoisomerases II. Furthermore, these results reveal that there are no direct relations between the DNA binding affinities of the two Ru^{II} complexes and their abilities to inhibit the activity of topoisomerases I and II. We hope that this work will aid in advancing our knowledge of the interaction between polypyridyl-based Ru^{II} complexes and DNA, as well as laying the foundation for the rational design of dual topoisomerases I and II inhibitors as novel anti-cancer agents.

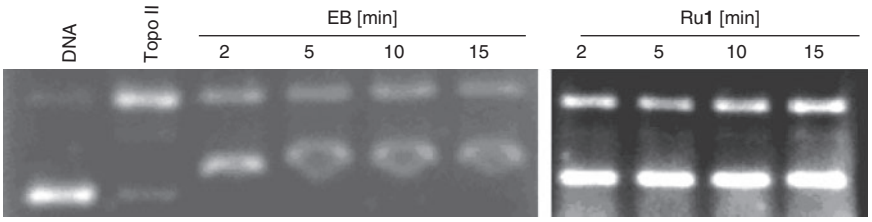

Fig. 11. The time dependence of Topo II DNA strand passage assays in the presence of ethidium bromide (EB) and Ru**1**.

Experimental

Reagents and Physical Measurements

All chemicals used were obtained from commercial sources and directly used without additional purification. 1,10-Phenanthroline-5,6-dione,[29] *cis*-$[Ru(phen)_2Cl_2]\cdot 2H_2O$,[30] 4-carbazol-9-yl-benzaldehyde, and 9-butyl-9*H*-carbazole-3,6-dicarbaldehyde[31] were synthesised according to the literature methods. Doubly distilled water was used to prepare buffers. CT-DNA was obtained from the Sino-American Biotechnology Co. A solution of CT-DNA in buffer gave a ratio of UV absorbance at 260 and 280 nm of ~1.8–1.9 : 1, indicating that the DNA was sufficiently free of protein.[32] The DNA concentration per nucleotide was determined by absorption spectroscopy using the molar absorption coefficient (6600 M^{-1} cm^{-1}) at 260 nm.[33] DNA Topo I from calf thymus together with human Topo IIα were purchased from TopoGen Inc.

Microanalyses (C, H and N) were carried out on a Perkin–Elmer 240Q elemental analyser. UV-Vis spectra were recorded with a PerkinElmer Lambda 25 spectrophotometer, emission spectra were recorded with a PerkinElmer LS 55 luminescence spectrometer at room temperature. ^{1}H NMR spectra were recorded on an Avance-400 spectrometer with d_6-DMSO as solvent at room temperature and tetramethylsilane as the internal standard. Mass spectrometry was measured on an Autoflex III Maldi-Tof mass spectrometer (Bruker) using DMSO as the mobile phase. The data of agarose gel electrophoresis were recorded on the FluorChem FC2.

DNA-Binding Experiments

The methods for spectroscopic titrations and viscosity measurements of Ru**1** and Ru**2** binding with CT-DNA were as published.[15] Using the McGheeeVon Hippel (MVH) model,[34] the intrinsic binding constants (K_b) of either Ru**1** or Ru**2** to CT-DNA were determined by monitoring the changes of absorbance at 351 nm for Ru**1** and 367 nm for Ru**2** upon addition of DNA.

Thermal DNA denaturation experiments were carried out with a Perkin–Elmer Lambda-25 spectrophotometer equipped with a Peltier temperature-control programmer (±0.1°C). The temperature of the solution was increased from 50 to 95°C at a rate of 1°C min^{-1}, and the absorbance at 260 nm was continuously monitored for solutions of CT-DNA (100 μM) in the absence and presence of the Ru^{II} complex (10 μM). The data were presented as $(A - A_0)/(A_f - A_0)$ versus temperature, where A_f, A_0, and A are the final, initial, and observed absorbance at 260 nm, respectively.

DNA Photocleavage Experiments

The DNA photocleavage experiments were carried out with a 10 μL total sample volume in 0.5 mL transparent Eppendorf tubes containing supercoiled pBR322 DNA (0.1 μg) and a variable concentration of Ru^{II} complexes (0–15 μM) in buffer B (50 mM TRIS-HCl, 18 mM NaCl, pH 7.2). Irradiation of the solutions was performed at room temperature with a UV lamp (365 nm, 10 W). Following irradiation, all the samples were analysed by 1 % agarose gel electrophoresis for 80 min at 75 V in buffer C (89 mM Tris, 89 mM boronhydroxide, 2 mM ethylenediaminetetraacetic acid). Gels were stained with EB (1 μg mL^{-1}) and then photographed and analysed on the FluorChem FC2.

Topoisomerase Inhibition Assay

Supercoiled pBR322 DNA (0.1 μg) was incubated with 1 unit of Topo I (one unit of the enzyme was defined as the amount that completely relaxes 1 μg of negatively supercoiled pBR322 DNA at 37°C in 30 min under the standard assay conditions) and variable concentrations of Ru^{II} complexes (0–15 μM) at 37°C for 30 min in buffer D (35 mM TRIS-HCl, pH 8.0, 2.5 mM dithiothreitol (DTT), 5 mM $MgCl_2$, 2 mM spermidine, 72 mM KCl, 0.1 μg mL^{-1} bovine serum albumin (BSA)), and the total reaction volume was 20 μL. Reactions were terminated by adding 4 μL of 5 × stop solution consisting of 0.25 % bromophenol blue, 45 % glycerol, and 4.5 % sodium dodecyl sulphate (SDS). DNA samples were then carried out through 1 % agarose in buffer C at 75 V for 2 h at room temperature. Gels were stained with EB (1 μg mL^{-1}), and photographed under the FluorChem FC2. The concentrations of the inhibitor that prevented 50 % of the supercoiled DNA from being converted into relaxed DNA (IC_{50} values) were calculated by the midpoint concentration for drug-induced DNA unwinding.

Topo II functional activity was assayed in buffer E (10 mM TRIS-HCl, 50 mM NaCl, 50 mM KCl, 5.0 mM $MgCl_2$, 0.1 mM Na_2H_2edta, 15 μg mL^{-1} BSA, 1.0 mM ATP, pH 7.9) containing 0.1 μg of pBR322 DNA and 2 units of Topo II in the absence and presence either Ru**1** or Ru**2**. The reaction mixture was incubated at 30°C for 15 min. Except for these, other subsequent operations were similar to the previous paragraph.

DNA Strand Passage Assay

The DNA strand passage activity of Topo I was determined by investigating the ability of Topo I to relax negatively supercoiled plasmid DNA or to supercoil plasmid DNA.[35,36] The reaction was carried out without drug or with 10 μM Ru^{II} complexes or EB in buffer D. Topo I was added after a 5 min incubation of DNA with drug or water, and reactions were incubated up to 15 min at 37°C. Reactions were stopped, processed, and subjected to gel electrophoresis as above.

Regarding the DNA strand passage activity of Topo II, reactions contained relaxed or supercoiled pBR322 plasmid DNA (0.3 μg) and 10 units of Topo II in buffer E. Following a 5 min incubation, Topo II was added and then reactions were

incubated up to 15 min at 30°C. The rest of the operations were the same as described above.

Synthesis of Cptcp

The procedure for the synthesis of ligand 2-(4-carbazol-9-yl-phenyl)-1*H*-1,3,7,8-tetraaza-cyclopenta-[*l*]-phenanthrene was carried out as below. A mixture of 1,10-phenanthroline-5,6-dione (0.42 g, 2.0 mM), 4-carbazol-9-yl-benzaldehyde (0.54 g, 2.0 mM), ammonium acetate (3.2 g, 42 mM), and glacial acetic acid (40 cm^3) was refluxed with stirring for 5 h, and then cooled to room temperature and diluted with water (60 mL). Dropwise addition of concentrated aqueous ammonia gave a yellow precipitate, which was collected and washed with distilled water, dichloromethane, and ethanol. The crude product was completely dissolved in ethanol and then purified by recrystallisation. The pure yellow crystalline solid was filtered from the solution and dried at 100°C under vacuum. Yield: 0.66 g, 72 %. Anal. Calc. for $C_{31}H_{19}N_5$: C 80.68, H 4.15, N 15.17. Found: C 80.79, H 4.26, N 15.01 %. *m*/*z* (MALDI-ToF, CH_3COOH) 461.96 ($[M + H]^+$).

Synthesis of Btcpc

The procedure for synthesising 9-butyl-6-(1*H*-1,3,7,8-tetraaza-cyclopenta- [*l*]phenanthren-2-yl)-9*H*-carbazole-3-carbaldehyde (btcpc) was similar to that for the preparation of cptcp, with 9-butyl-9H-carbazole-3,6-dicarbaldehyde (0.11 g, 0.40 mM) in place of 4-carbazol-9-yl-benzaldehyde. Yield: 0.14 g, 75 %. Anal. Calc. for $C_{30}H_{23}N_5O$: C 76.74, H 4.94, N 14.92. Found: C 76.81, H 4.98, N 14.85 %. *m*/*z* (MALDI-ToF, CH_3COOH) 470.24 ($[M + H]^+$).

*Synthesis of [Ru(phen)$_2$(cptcp)](ClO$_4$)$_2$·2H$_2$O (Ru**1**)*

A mixture of *cis*-$[Ru(phen)_2Cl_2]\cdot 2H_2O$ (0.14 mg, 0.25 mM), cptcp (0.12 g, 0.25 mM), ethanol (16 mL), and H_2O (4 mL) was thoroughly deoxygenated and then refluxed for 9 h under nitrogen. The solution was cooled to room temperature and was filtered to remove the insoluble substance. An orange precipitate was obtained by dropwise addition of a 4-fold excess of saturated aqueous sodium perchlorate solution. The precipitate was collected and washed with small amounts of water, ethanol, and diethyl ether, and then dried under vacuum at 50°C. Purification by chromatography on a neutral alumina column with a mixture of acetonitrile and methylbenzene (1 : 1, v/v) as eluant yielded 0.19 g, 67 %. Anal. Calc. for $C_{55}H_{39}N_9Cl_2O_{10}Ru$: C 57.05, H 3.39, N 10.89. Found: C 56.92, H 3.57, N 10.69 %. δ_H (400 MHz, d_6-DMSO) 14.61 (s, 1H), 9.13 (d, *J* 6.8, 2H), 8.81 (s, 4H), 8.70 (d, *J* 6.8, 2H), 8.64 (d, *J* 6.8, 2H), 8.41 (s, 4H), 8.32 (d, *J* 6.4, 2H), 8.18 (s, 4H), 7.98–8.09 (m, 6H), 7.80 (s, 2H), 7.51–7.63 (m, 4H), 7.37 (d, *J* 6.0, 2H). *m*/*z* (MALDI-ToF, CH_3CN) 922.1 ($[M - 2ClO_4 - H]^+$).

*Synthesis of [Ru(phen)$_2$(btcpc)](ClO$_4$)$_2$·2H$_2$O (Ru**2**)*

The procedure for Ru**2** was similar to that for the preparation of Ru**1**, except that btcpc (96 mg, 0.2 mM) was used instead of cptcp. Yield: 189 mg, 62 %. Anal. Calc. for $C_{54}H_{43}N_9Cl_2O_{11}Ru$: C 55.63. H 3.72, N 10.81. Found: C 55.42, H 3.93, N 10.65 %. δ_H (400 MHz, d_6-DMSO) 14.42 (s, 1H), 10.14 (s, 1H), 9.24 (s, 1H), 9.24 (s, 2H), 9.13 (d, *J* 6.0, 2H), 8.90 (s, 2H), 8.79 (d, *J* 7.2, 4H), 8.52 (d, *J* 8.0, 2H), 8.41 (s, 4H), 8.09 (t, J_1 22.8, J_2 27.2, 4H), 8.10–8.03 (m, 5H), 7.92 (d, *J* 7.2, 2H), 7.84–7.79 (m, 4H), 4.59 (s, 2H), 1.85 (s, 2H), 1.35 (s, 2H), 0.92 (s, 3H). *m*/*z* (MALDI-ToF, CH_3CN) 930.3 ($[M - 2ClO_4 - H]^+$).

Supplementary Material

MALDI-TOF mass spectrometry, ^{1}H NMR spectra, absorption spectrum and fluorescence spectra of Ru**1** and Ru**2**, effects of different concentrations of Ru**2** on the activity of DNA Topo I/II, and the time dependence of Topo II DNA strand passage assays in the presence of Ru**2** are available on the Journal's website.

Acknowledgements

The authors are grateful for the support of the National Natural Science Foundation of the People's Republic of China (21071120), the Scientific Research Foundation of Hunan Provincial Education Department (11A117), Hunan Provincial Natural Science Foundation of China (12JJ2011) and the Key Project of Chinese Ministry of Education (212127). They also thank the reviewers for the comments that enabled them to improve upon the manuscript.

References

[1] (a) J. M. Berger, S. J. Gamblin, S. C. Harrison, J. C. Wang, *Nature* **1996**, *379*, 225. doi:10.1038/379225A0
(b) J. C. Wang, *Annu. Rev. Biochem.* **1996**, *65*, 635. doi:10.1146/ANNUREV.BI.65.070196.003223

[2] (a) A. Y. Chen, L. F. Liu, *Annu. Rev. Pharmacol. Toxicol.* **1994**, *34*, 191. doi:10.1146/ANNUREV.PA.34.040194.001203
(b) J. J. Champoux, *Annu. Rev. Biochem.* **2001**, *70*, 369. doi:10.1146/ANNUREV.BIOCHEM.70.1.369

[3] J. C. Wang, *Nat. Rev. Mol. Cell Biol.* **2002**, *3*, 430. doi:10.1038/NRM831

[4] S. Salerno, F. D. Settimo, S. Taliani, F. Simorini, C. L. Motta, G. Fornaciari, A. M. Marini, *Curr. Med. Chem.* **2010**, *17*, 4270. doi:10.2174/092986710793361252

[5] (a) J. A. Holden, *Curr. Med. Chem.* **2001**, *1*, 1.
(b) J. L. Nitiss, *Nat. Rev. Cancer* **2009**, *9*, 338. doi:10.1038/NRC2607

[6] (a) H. K. Wang, S. L. Morris-Natschke, K. H. Lee, *Med. Res. Rev.* **1997**, *17*, 367. doi:10.1002/(SICI)1098-1128(199707)17:4<367::AID-MED3>3.0.CO;2-U
(b) D. F. Kehrer, O. Soepenberg, W. J. Loos, J. Verweij, A. Sparreboom, *Anticancer Drugs* **2001**, *12*, 89. doi:10.1097/00001813-200102000-00002
(c) H. Jensen, A. V. Thougaard, M. Grauslund, B. Søkilde, E. V. Carstensen, H. K. Dvinge, D. A. Scudiero, P. B. Jensen, R. H. Shoemaker, M. Sehested, *Cancer Res.* **2005**, *65*, 7470. doi:10.1158/0008-5472.CAN-05-0707
(d) N. Dias, H. Vezin, A. Lansiaux, C. Bailly, *Top. Curr. Chem.* **2005**, *253*, 89.
(e) A. Morrell, M. Placzek, S. Parmley, S. Antony, T. S. Dexheimer, Y. Pommier, M. Cushman, *J. Med. Chem.* **2007**, *50*, 4419. doi:10.1021/JM070361Q
(f) R. Gaur, L. Mishra, *Inorg. Chem.* **2012**, *51*, 3059. doi:10.1021/IC202440R

[7] (a) M. Chandra, A. N. Sahay, D. S. Pandey, R. P. Tripathi, J. K. Saxena, V. J. M. Reddy, M. C. Puerta, P. J. Valerga, *J. Organomet. Chem.* **2004**, *689*, 2256. doi:10.1016/J.JORGANCHEM.2004.03.044
(b) S. K. Singh, S. Joshi, A. R. Singh, J. K. Saxena, D. S. Pandey, *Inorg. Chem.* **2007**, *46*, 10869. doi:10.1021/IC700885M
(c) X. Chen, F. Gao, W. Y. Yang, J. Sun, Z. X. Zhou, L. N. Ji, *Inorg. Chim. Acta* **2011**, *378*, 140. doi:10.1016/J.ICA.2011.08.047
(d) Y. C. Lo, T. P. Ko, W. C. Su, T. L. Su, A. H. Wang, *J. Inorg. Biochem.* **2009**, *103*, 1082. doi:10.1016/J.JINORGBIO.2009.05.006
(e) X. Chen, F. Gao, Z. X. Zhou, W. Y. Yang, L. T. Guo, L. N. Ji, *J. Inorg. Biochem.* **2010**, *104*, 576. doi:10.1016/J.JINORGBIO.2010.01.010

[8] (a) B. M. Zeglis, V. C. Pierrea, J. K. Barton, *Chem. Commun.* **2007**, *44*, 4565. doi:10.1039/B710949K
(b) C. A. Puckett, R. J. Erns, J. K. Barton, *Dalton Trans.* **2010**, *39*, 1159. doi:10.1039/B922209J
(c) M. R. Gill, J. A. Thomas, *Chem. Soc. Rev.* **2012**, *41*, 3179. doi:10.1039/C2CS15299A

[9] (a) W. A. Denny, *Expert Opin. Investig. Drugs* **1997**, *6*, 1845. doi:10.1517/13543784.6.12.1845
(b) T. Simon, A. Langler, F. Berthold, T. Klingebiel, B. Hero, *J. Pediatr. Hematol. Oncol.* **2007**, *29*, 101. doi:10.1097/MPH.0B013E3180320B48
(c) H. J. Choi, B. C. Cho, S. J. Shin, S. H. Cheon, J. Y. Jung, J. Chang, S. K. Kim, J. H. Sohn, J. H. Kim, *Cancer Chemother. Pharmacol.* **2008**, *61*, 309. doi:10.1007/S00280-007-0505-9
(d) B. Saraiya, M. Gounder, J. Dutta, A. Saleem, C. Collazo, L. Zimmerman, A. Nazar, M. Gharibo, D. Schaar, Y. Lin, W. Shih, J. Aisner, R. K. Strai, E. H. Rubin, *Anticancer Drugs* **2008**, *19*, 411. doi:10.1097/CAD.0B013E3282F5218B

[10] (a) F. Gao, H. Chao, J. Q. Wang, Y. X. Yuan, B. Sun, Y. F. Wei, B. Pen, L. N. Ji, *J. Biol. Inorg. Chem.* **2007**, *12*, 1015. doi:10.1007/S00775-007-0272-4
(b) S. Sharma, S. K. Singh, D. S. Pandey, *Inorg. Chem.* **2008**, *47*, 1179. doi:10.1021/IC701518E
(c) F. Gao, H. Chao, F. Zhou, X. Chen, Y. F. Wei, K. Z. Zheng, L. N. Ji, *J. Inorg. Biochem.* **2008**, *102*, 1050. doi:10.1016/J.JINORGBIO.2007.12.025
(d) P. Kumar, A. K. Singh, J. K. Saxena, D. S. Pandey, *J. Organomet. Chem.* **2009**, *694*, 3570. doi:10.1016/J.JORGANCHEM.2009.07.014

[11] J. F. Kou, C. Qian, J. Q. Wang, X. Chen, L. L. Wang, H. Chao, L. N. Ji, *J. Biol. Inorg. Chem.* **2012**, *17*, 81. doi:10.1007/S00775-011-0831-6

[12] E. A. Steck, A. R. Day, *J. Am. Chem. Soc.* **1943**, *65*, 452. doi:10.1021/JA01243A043

[13] J. G. Liu, Q. L. Zhan, L. N. Ji, *Transit. Metal Chem.* **2001**, *26*, 733. doi:10.1023/A:1012037312390

[14] J. Z. Wu, B. H. Ye, L. Wang, L. N. Ji, J. Y. Zhou, R. H. Li, Z. Y. Zhou, *J. Chem. Soc., Dalton Trans.* **1997**, *8*, 1395. doi:10.1039/A605269J

[15] L. F. Tan, J. L. Shen, J. Liu, L. L. Zeng, L. H. Jin, C. Weng, *Dalton Trans.* **2012**, *41*, 4575. doi:10.1039/C2DT12402E

[16] F. Gao, H. Chao, F. Zhou, Y. X. Yuan, B. Peng, L. N. Ji, *J. Inorg. Biochem.* **2006**, *100*, 1487. doi:10.1016/J.JINORGBIO.2006.04.008

[17] J. G. Liu, Q. L. Zhang, X. F. Shi, L. N. Ji, *Inorg. Chem.* **2001**, *40*, 5045. doi:10.1021/IC001124F

[18] J. B. Lepecq, C. Paoletti, *J. Mol. Biol.* **1967**, *27*, 87. doi:10.1016/0022-2836(67)90353-1

[19] J. L. Morgan, D. P. Buck, A. G. Turley, J. G. Collins, F. R. Keene, *Inorg. Chim. Acta* **2006**, *359*, 888. doi:10.1016/J.ICA.2005.06.036

[20] S. Shi, J. Zhao, X. T. Geng, T. M. Yao, H. L. Huang, T. L. Liu, L. F. Zheng, Z. H. Liu, D. J. Yang, L. N. Ji, *Dalton Trans.* **2010**, *39*, 2490. doi:10.1039/B916094A

[21] S. Satyanarayana, J. C. Dabroniak, J. B. Chaires, *Biochemistry* **1992**, *31*, 9319. doi:10.1021/BI00154A001

[22] E. Tselepi-Kalouli, N. Katsaros, *J. Inorg. Biochem.* **1989**, *37*, 271. doi:10.1016/0162-0134(89)85002-0

[23] (a) J. Waring, *J. Mol. Biol.* **1965**, *13*, 269. doi:10.1016/S0022-2836(65)80096-1
(b) G. A. Neyhart, N. Grover, S. R. Smith, W. A. Kalsbeck, T. A. Fairly, M. Cory, H. H. Thorp, *J. Am. Chem. Soc.* **1993**, *115*, 4423. doi:10.1021/JA00064A001
(c) S. Shi, T. Xie, T. M. Yao, C. R. Wang, X. T. Geng, D. J. Yang, L. J. Han, L. N. Ji, *Polyhedron* **2009**, *28*, 1355. doi:10.1016/J.POLY.2009.02.035

[24] J. K. Barton, A. L. Raphael, *J. Am. Chem. Soc.* **1984**, *106*, 2466. doi:10.1021/JA00320A058

[25] G. Cohen, H. Eisenberg, *Biopolymers* **1969**, *8*, 45. doi:10.1002/BIP.1969.360080105

[26] H. Y. Mei, J. K. Barton, *Proc. Natl. Acad. Sci. USA* **1988**, *85*, 1339. doi:10.1073/PNAS.85.5.1339

[27] J. M. Fortune, L. Velea, D. E. Graves, T. Utsugi, Y. Yamada, N. Osheroff, *Biochemistry* **1999**, *38*, 15580. doi:10.1021/BI991792G

[28] K. J. Du, J. Q. Wang, J. F. Kou, G. Y. Li, L. L. Wang, H. Chao, L. N. Ji, *Eur. J. Med. Chem.* **2011**, *46*, 1056. doi:10.1016/J.EJMECH.2011.01.019

[29] M. Yamada, Y. Tanaka, Y. Yoshimato, S. Kuroda, I. Shimao, *Bull. Chem. Soc. Jpn.* **1992**, *65*, 1006. doi:10.1246/BCSJ.65.1006

[30] B. P. Sullivan, D. J. Salmon, T. J. Meyer, *Inorg. Chem.* **1978**, *17*, 3334. doi:10.1021/IC50190A006

[31] X. M. Wang, Y. F. Zhou, W. T. Yu, C. Wang, Q. Fang, M. H. Jiang, H. Lei, H. Z. Wang, *J. Mater. Chem.* **2000**, *10*, 2698. doi:10.1039/B006764O

[32] J. Marmur, *J. Mol. Biol.* **1961**, *3*, 208. doi:10.1016/S0022-2836(61)80047-8

[33] M. F. Reichmann, S. A. Rice, C. A. Thomas, P. Doty, *J. Am. Chem. Soc.* **1954**, *76*, 3047. doi:10.1021/JA01640A067

[34] M. T. Carter, M. Rodriguez, A. Bard, *J. Am. Chem. Soc.* **1989**, *111*, 8901. doi:10.1021/JA00206A020

[35] N. Osheroff, E. R. Shelton, D. L. Brutlag, *J. Biol. Chem.* **1983**, *258*, 9536.

[36] J. M. Fortune, N. Osheroff, *J. Biol. Chem.* **1998**, *273*, 17643. doi:10.1074/JBC.273.28.17643